MODEL CALIBRATION

To demonstrate how to calibrate the above proposed model framework, this study uses the field data collected from small-scale field experiments of a connected autonomous vehicle (CAV) mandatory lane changing (LC) model with three surrounding human driven vehicles (HVs) in a previous study (Wang et al., 2020).

The test track segment is a two-lane straight road with length $L = 800$ m and lane width $D = 3.5$ m. Figure 1 shows the field experiment of the CAV mandatory LC with 3 surrounding HVs. All vehicles' lengths are set as $C = 4.6$ m. The sine-function based LC path is implemented during the field experiments. Videos of the field experiments are available at https://www.youtube.com/watch?v=34FubITFebI. Sample data are available at https://github.com/sgzzgit/Autonomous-Vehicle-Lane-Change-Experiment-Data.

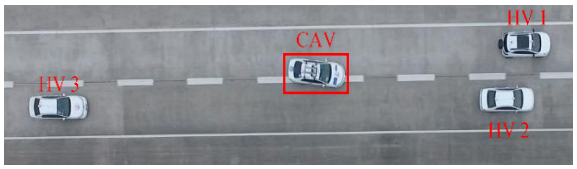

Source: https://www.youtube.com/watch?v=34FubITFebI

Figure 1. Bird view of the field experiment.

The CAV mandatory LC model flow chart is presented in Figure 2. This chart is just a simplification of the proposed CAV LC model in the mandatory LC context. In the field experiments, the CAV used the ACC model to follow HVs 1 and 2, and continuously checked the safety criterion considering HV 2 and HV 3. Once the safety criterion was met, a sine-function-based LC path was generated for the CAV to follow. The safety criterion was continuously checked in the LC path following process, and the LC maneuver was aborted if the safety criterion failed to be met before the CAV crossed the lane marking. When the CAV reached the target position, i.e., the center line of the target lane, it successfully made an automated LC.

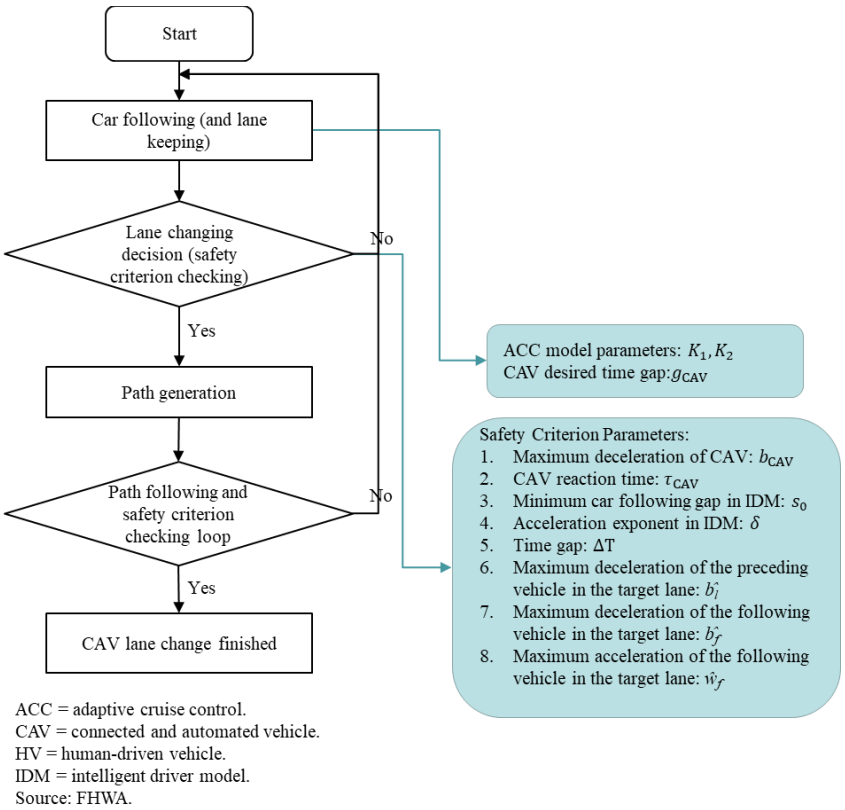

ACC = adaptive cruise control.
CAV = connected and automated vehicle.
HV = human-driven vehicle.
IDM = intelligent driver model.
Source: FHWA.

Figure 2. Connected and automated vehicle mandatory lane-changing logic with key parameters.

Four cases ($c \in \{1, 2, 3, 4\}$) of experiments representing four different traffic situations were conducted.

- In the first case (c = 1), the preceding vehicle in the current lane (i.e., HV 1 in Figure 1) was asked to decelerate, creating a shock wave. The preceding vehicle in the target lane (i.e., HV 2 in Figure 1) kept a relatively constant speed and the following vehicle in the target lane (i.e., HV 3 in Figure 1) was not aggressive, yielding to the CAV LC.
- In the second case (c = 2), HV 2 was asked to decelerate, creating a shock wave. HV 1 kept relatively constant speed and HV 3 was not aggressive, yielding to the CAV LC.
- In the third case (c = 3), HVs 1 and 2 both kept relatively constant speed and HV 3 was not aggressive, yielding to the CAV LC.
- In the final case (c = 4), HVs 1 and 2 both kept relatively constant speed, but HV 3 was accelerating instead of yielding to the CAV LC, which represented aggressive driving; this forced the CAV to abort the LC maneuver.

The speeds of HV 1 and HV 2 were kept within 9–41 ft/s during the experiments (Wang et al., 2020). Note that two runs of the experiments with the same settings were conducted for each case. The data from the first run of four cases were used for simulation model calibration; the second run data were used for simulation model validation. Small-scale simulation with the same setting as the field experiments was conducted to calibrate the CAV mandatory LC model parameters (listed in Figure 2), a component of the mixed traffic simulation model. HVs 1, 2, and 3 trajectories were controlled to replicate the field experiment trajectories and the CAV trajectory was generated using the proposed CAV LC model. RMSE of the CAV longitudinal positions was formulated as:

$$RMSE_c^x(\beta) = \sqrt{\frac{1}{Q_c}\sum_{q=1}^{Q_c}\left(x_{c,q}^{obs} - x_{c,q}^{cal}(\beta)\right)^2}$$

Where:
$x_{c,q}^{obs}$, $x_{c,q}^{cal}$ = field-observed and calibrated longitudinal positions of the CAV at time point q in case c with unit ft.
Q_c = total number of time points in case c.
β = parameters set.
ft = foot.
The error between the calibrated LC time point and field-observed LC time point was formulated as:

$$E_c^t(\beta) = |t_c^{LCobs} - t_c^{LCcal}(\beta)|$$

Where:
t_c^{LCobs}, t_c^{LCcal} = field-observed and calibrated LC time points in case c with unit s.
β = parameters set.
s = second.
Thus, the calibration optimization objective was formulated as:

$$\min_{\beta} \frac{1}{4}\sum_{c=1}^{4}\left(RMSE_c^x(\beta) + E_c^t(\beta)\right)$$

Where:
$RMSE_c^x$ = root mean square error of the CAV longitudinal positions in case c.
E_c^t = error between the calibrated LC time point and field-observed LC time point in case c.
β = parameters set.
RMSE of the CAV speeds was also calculated to measure the calibration results, formulated as:

$$RMSE_c^v(\beta) = \sqrt{\frac{1}{Q_c}\sum_{q=1}^{Q_c}\left(v_{c,q}^{obs} - v_{c,q}^{cal}(\beta)\right)^2}$$

Where:
$v_{c,q}^{obs}$, $v_{c,q}^{cal}$ = field-observed and calibrated speeds of the CAV at time point q in case c with unit ft/s.

Q_c = total number of time points in case c.
β = parameters set.
ft/s = foot per second.
The interior-point method was used to find the optimal parameter values. As shown in Figure 3, the objective function value was stable at 6.19 after iteration 7 with an average $RMSE_c^x(\beta)$ of 4.79 ft and an average $E_c^t(\beta)$ of 1.4 s, indicating a good calibration result (shown in Table 1). The parameters β calibration results are provided in Table 2. The detailed CAV longitudinal positions, speeds, and LC time calibration results of four cases are provided in Figure 4, Figure 5, Figure 6, and Figure 7. The calibrated CAV trajectories (i.e., the dashed curves) were almost consistent with the field-observed trajectories (i.e., the solid curves) with minor differences with an average $RMSE_c^x(\beta)$ value of 4.79 ft and an average $E_c^t(\beta)$ value of 1.18 ft/s. The difference between the calibrated and field-observed LC time point was less than 3 s across all cases.

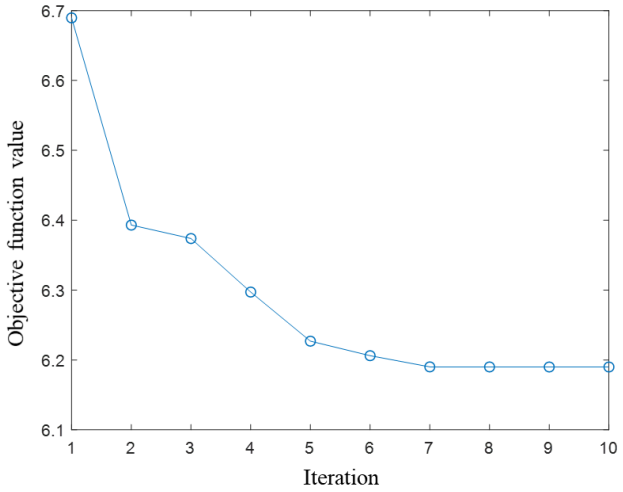

Source: FHWA.

Figure 3. Graph. Calibration objective function convergence.

Table 1. Calibration results summary.

Case	t_c^{LCobs} (s)	t_c^{LCcal} (s)	E_c^t (s)	$RMSE_c^x$ (ft)	$RMSE_c^v$ (ft/s)
c = 1	36.2	39.0	2.8	6.10	1.80
c = 2	11.5	13.4	1.9	3.48	1.28
c = 3	30.2	31.1	0.9	3.02	0.66
c = 4	inf	inf	0.0	6.53	0.98
Average	\	\	1.4	4.79	1.18

inf = no lane-changing behavior. ft = foot. ft/s = foot per second. *RMSE* = root mean square error. s = second. t_c^{LCobs} = field-observed lane-changing time point in case c. t_c^{LCcal} = calibrated lane-changing time point in case c. E_c^t = error between the calibrated lane-changing time point and field-observed lane-changing time point. $RMSE_c^x$ = root mean square error of the connected and automated vehicle calibrated longitudinal positions. $RMSE_c^v$ = root mean square error of the connected and automated vehicle calibrated speeds. \ = not applicable.

Table 2. Parameters calibration results.

Parameters β	Calibration Results
K_1(s^{-2})	0.1997
K_2(s^{-1})	0.6820
g_{CAV}(s)	1.5265
b_{CAV}(ft/s^2)	-14.7600
τ_{CAV}(s)	0.9000
s_0(ft)	13.1324
δ	2.0000
ΔT(s)	1.3000
$\hat{b_l}$ / $\hat{b_f}$(ft/s^2)	-13.7795
$\hat{w_f}$(ft/s^2)	13.1234

b_{CAV} = CAV maximum deceleration rate. $\hat{b_l}$ = maximum deceleration of the preceding vehicle in the target lane. $\hat{b_f}$ = maximum deceleration of the following vehicle in the target lane. ft = foot. ft/s^2 = foot per second squared. g_{CAV} = CAV desired time gap. K_1, K_2 = adaptive cruise control model parameter. s = second. s_0 = minimum car-following gap in intelligent driver model. $\hat{w_f}$ = maximum acceleration of the following vehicle in the target lane. ΔT = time gap in intelligent driver model. δ = acceleration exponent in intelligent driver model. τ_{CAV} = CAV reaction time.

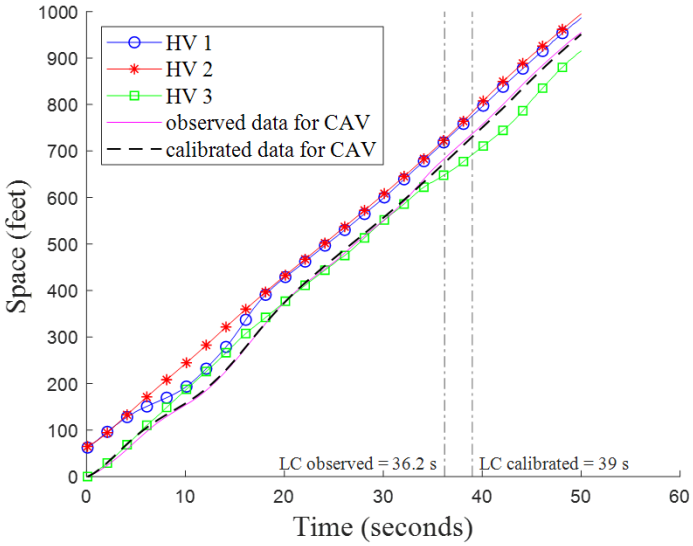

CAV = connected and automated vehicle.
HV = human-driven vehicle.
LC = lane changing.
Source: FHWA.

(a) Vehicle trajectories in case 1.

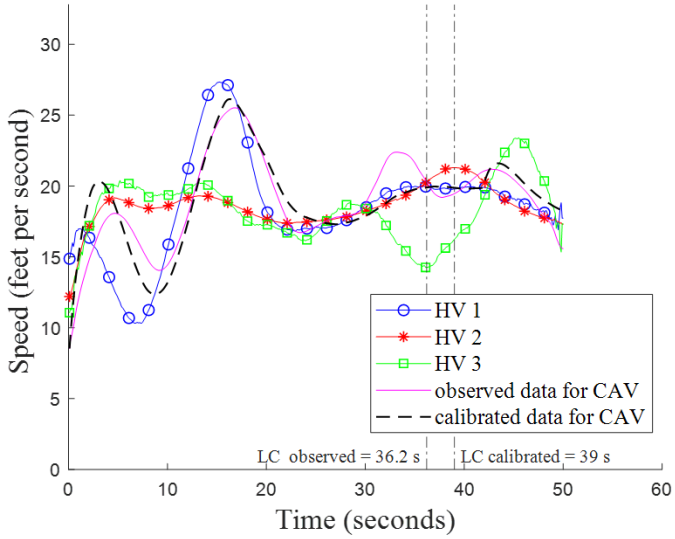

CAV = connected and automated vehicle.
HV = human-driven vehicle.
LC = lane changing.
Source: FHWA.

(b) Vehicle speeds in case 1.

Figure 4. Graph. Calibration results of case 1.

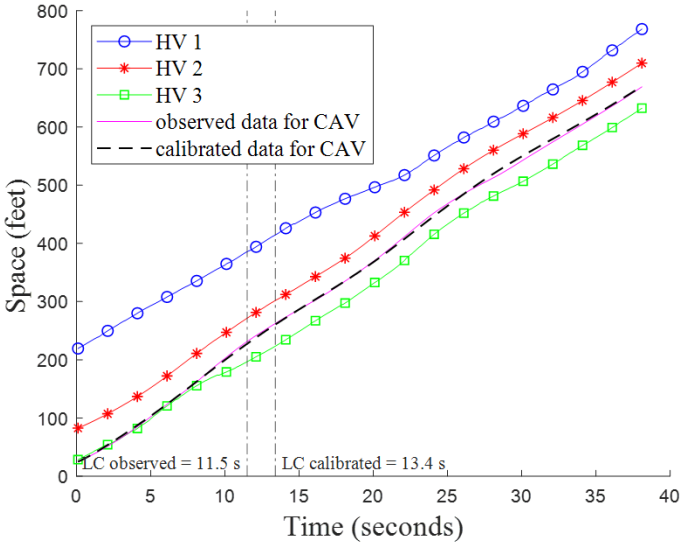

CAV = connected and automated vehicle.
HV = human-driven vehicle.
LC = lane changing.
Source: FHWA.

(a) Vehicle trajectories in case 2.

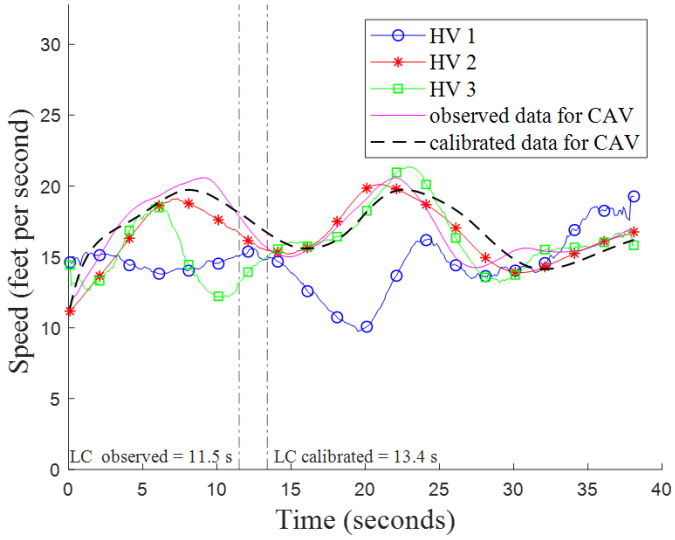

CAV = connected and automated vehicle.
HV = human-driven vehicle.
LC = lane changing.
Source: FHWA.

(b) Vehicle speeds in case 2.

Figure 5. Graph. Calibration results of case 2.

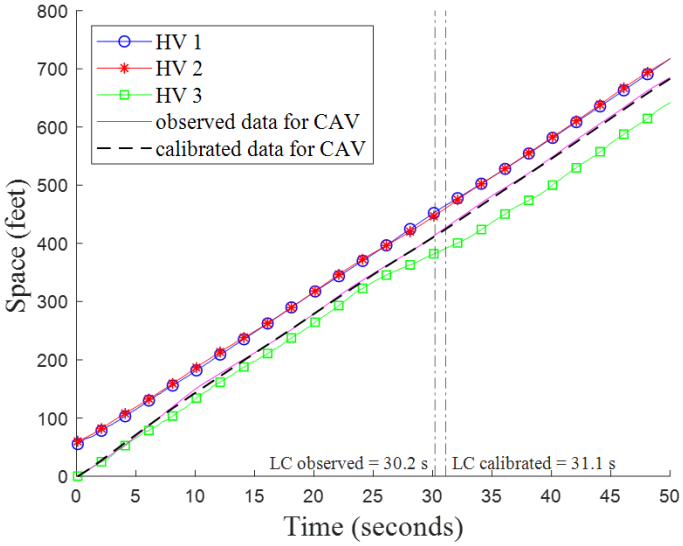

CAV = connected and automated vehicle.
HV = human-driven vehicle.
LC = lane changing.
Source: FHWA.

(a) Vehicle trajectories in case 3.

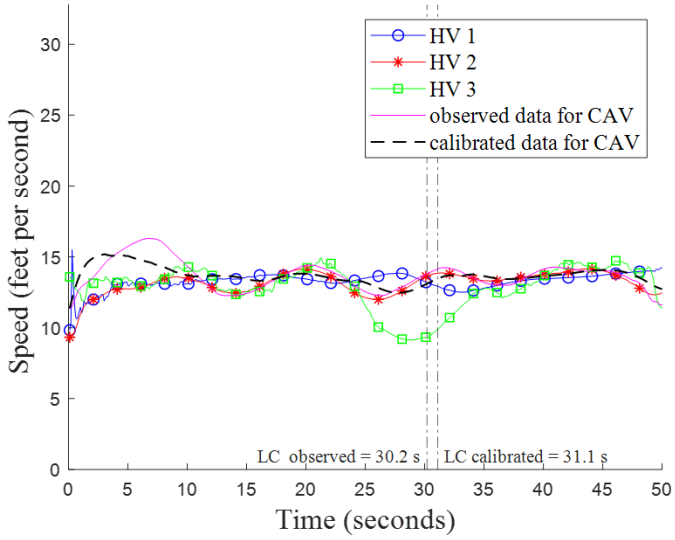

CAV = connected and automated vehicle.
HV = human-driven vehicle.
LC = lane changing.
Source: FHWA.

(b) Vehicle speeds in case 3.

Figure 6. Graph. Calibration results of case 3.

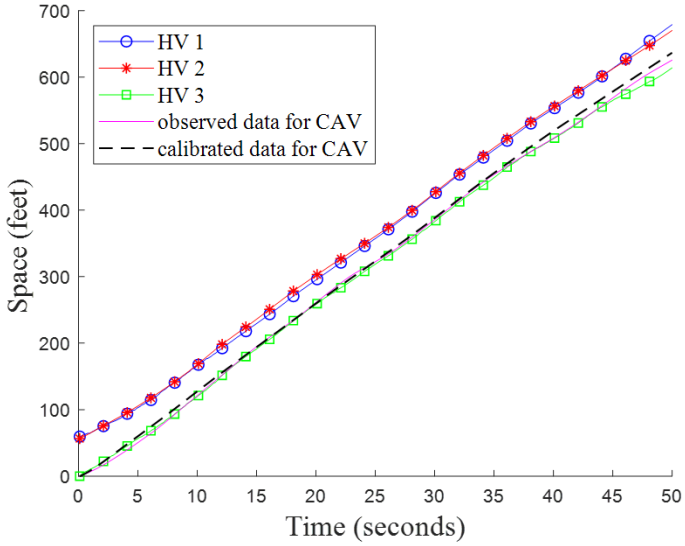

CAV = connected and automated vehicle.
HV = human-driven vehicle.
LC = lane changing.
Source: FHWA.

(a) Vehicle trajectories in case 4.

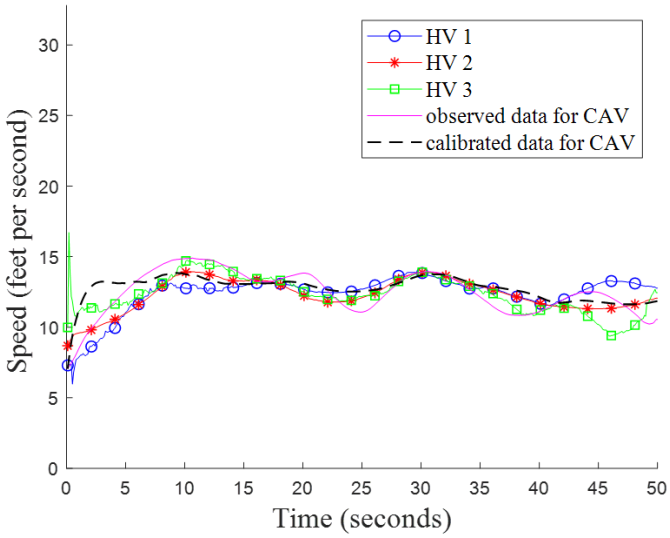

CAV = connected and automated vehicle.
HV = human-driven vehicle.
LC = lane changing.
Source: FHWA.

(b) Vehicle speeds in case 4.

Figure 7. Graph. Calibration results of case 4.

MODEL VALIDATION

The second run data of the four cases were used for model validation. RMSE of CAV longitudinal positions $RMSE_c^x$ and speeds $RMSE_c^v$ were calculated for four cases using the calibrated parameters from the first run.

$$RMSE_c^x(\beta) = \sqrt{\frac{1}{Q_c}\sum_{q=1}^{Q_c}\left(x_{c,q}^{obs} - x_{c,q}^{val}(\beta)\right)^2}$$

$$RMSE_c^v(\beta) = \sqrt{\frac{1}{Q_c}\sum_{q=1}^{Q_c}\left(v_{c,q}^{obs} - v_{c,q}^{val}(\beta)\right)^2}$$

Where:

$x_{c,q}^{obs}$, $x_{c,q}^{val}$ = field-observed and validated longitudinal positions of the CAV at time point q in case c with unit ft.

$v_{c,q}^{obs}$, $v_{c,q}^{val}$ = field-observed and validated speeds of the CAV at time point q in case c with unit ft/s.

Q_c = total number of time points in case c.

β = parameters set.

The validation results are summarized in Table 3. The error between the validated LC time and field observed LC time was only 0.53 s on average. $RMSE_c^x$ had an average value of 6.89 ft. Compared with the calibration results (i.e., the LC time error with an average value of 1.4 s and $RMSE_c^x$ with an average value of 4.79 ft), the validation results showed less difference, which suggested a valid calibration. Detailed validation results are provided in Figure 8, Figure 9, Figure 10, and Figure 11.

Table 3. Validation results summary.

Case	t_c^{LCobs} (s)	t_c^{LCval} (s)	E_c^t (s)	$RMSE_c^x$ (ft)	$RMSE_c^v$ (ft/s)
c = 1	53.6	53.8	0.2	5.09	0.82
c = 2	26.0	26.2	0.6	6.14	1.44
c = 3	21.3	22.6	1.3	6.14	1.05
c = 4	inf	inf	0.0	10.24	1.25
Average	\	\	0.53	6.89	1.15

inf = no lane-changing behavior. ft = foot. ft/s = foot per second. *RMSE* = root mean square error. s = second. t_c^{LCobs} = field-observed lane-changing time point in case c. t_c^{LCval} = validated lane-changing time point in case c. E_c^t = error between the validated lane-changing time point and field-observed lane-changing time point. $RMSE_c^x$ = root mean square error of the connected and automated vehicle validated longitudinal positions. $RMSE_c^v$ = root mean square error of the connected and automated vehicle validated speeds. \ = not applicable.

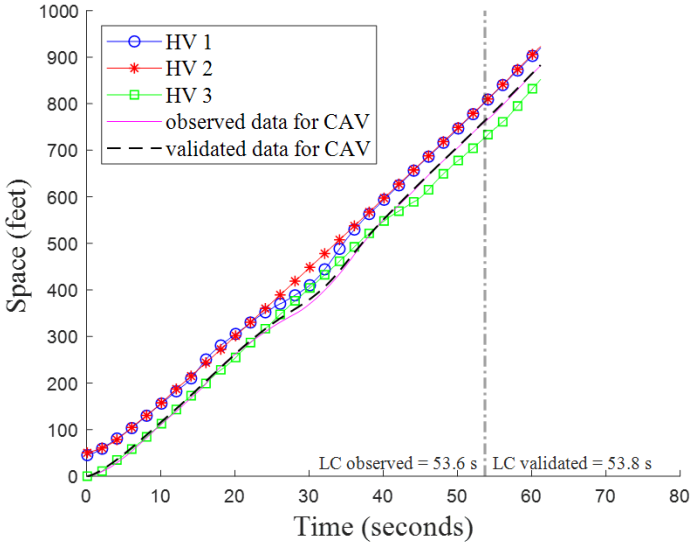

CAV = connected and automated vehicle.
HV = human-driven vehicle.
LC = lane changing.
Source: FHWA.

(a) Vehicle trajectories in case 1.

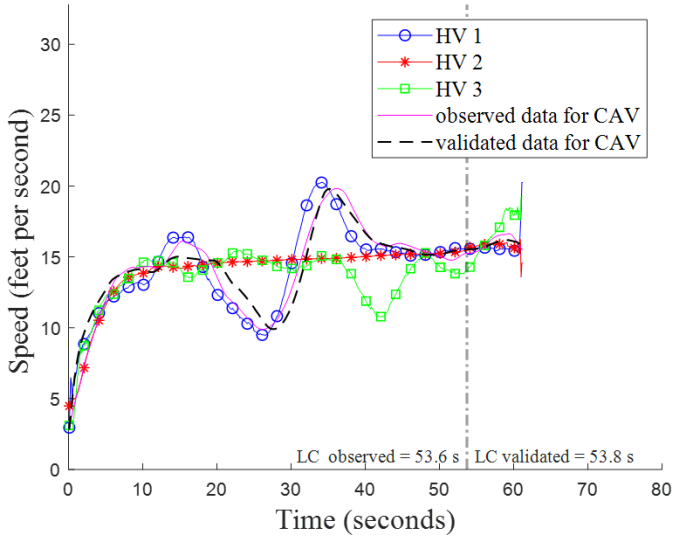

CAV = connected and automated vehicle.
HV = human-driven vehicle.
LC = lane changing.
Source: FHWA.

(b) Vehicle speeds in case 1.

Figure 8. Graph. Validation results of case 1.

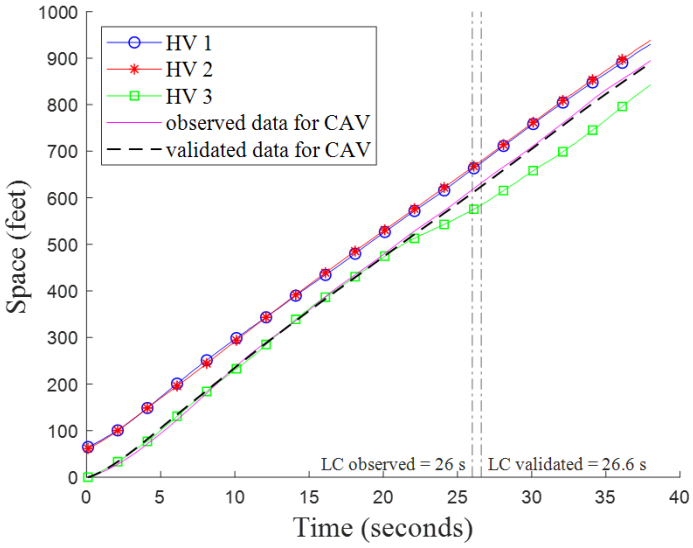

CAV = connected and automated vehicle.
HV = human-driven vehicle.
LC = lane changing.
Source: FHWA.

(a) Vehicle trajectories in case 2.

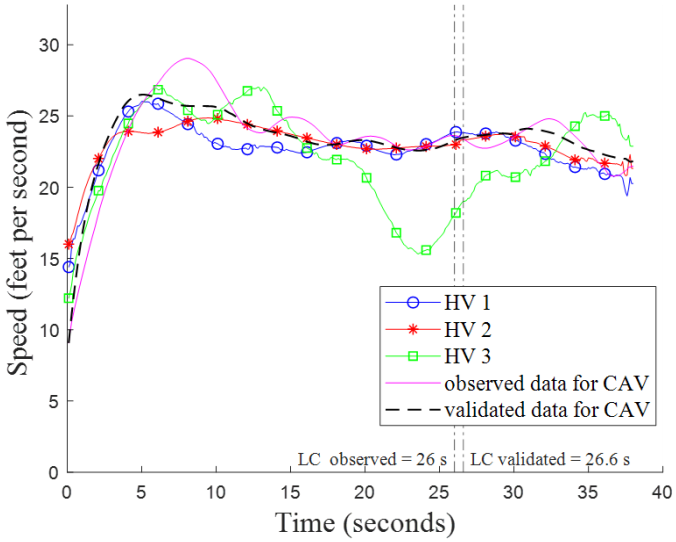

(b) Vehicle speeds in case 2.

Figure 9. Graph. Validation results of case 2.

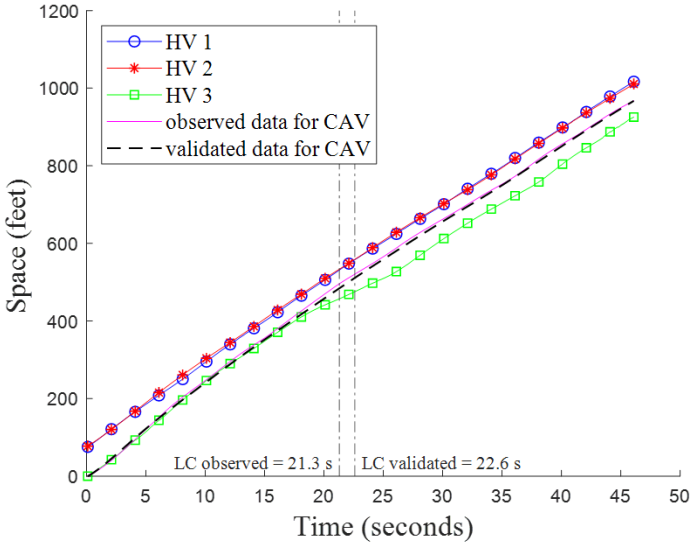

CAV = connected and automated vehicle.
HV = human-driven vehicle.
LC = lane changing.
Source: FHWA.

(a) Vehicle trajectories in case 3.

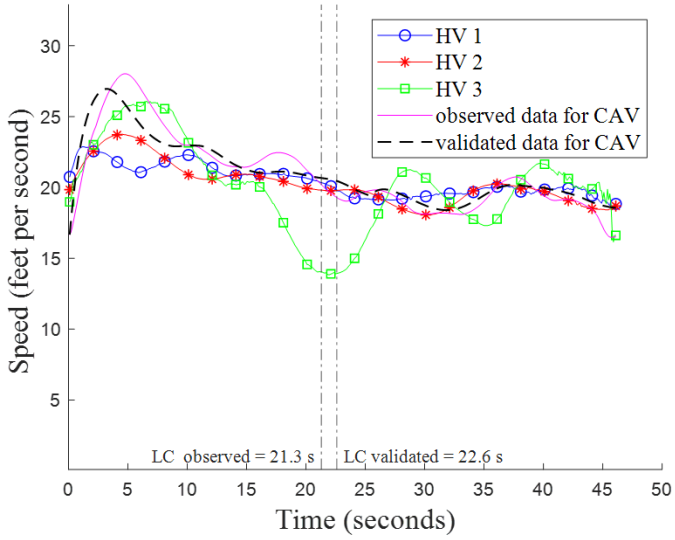

CAV = connected and automated vehicle.
HV = human-driven vehicle.
LC = lane changing.
Source: FHWA.

(b) Vehicle speeds in case 3.

Figure 10. Graph. Validation results of case 3.

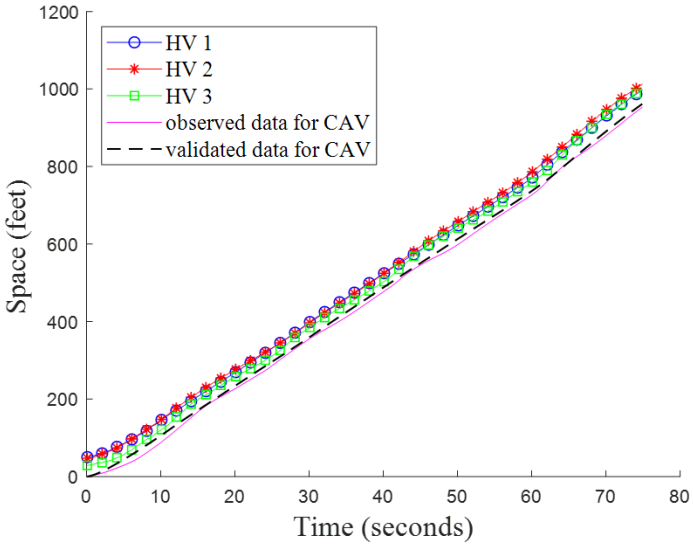

CAV = connected and automated vehicle.
HV = human-driven vehicle.
LC = lane changing.
Source: FHWA.

(a) Vehicle trajectories in case 4.

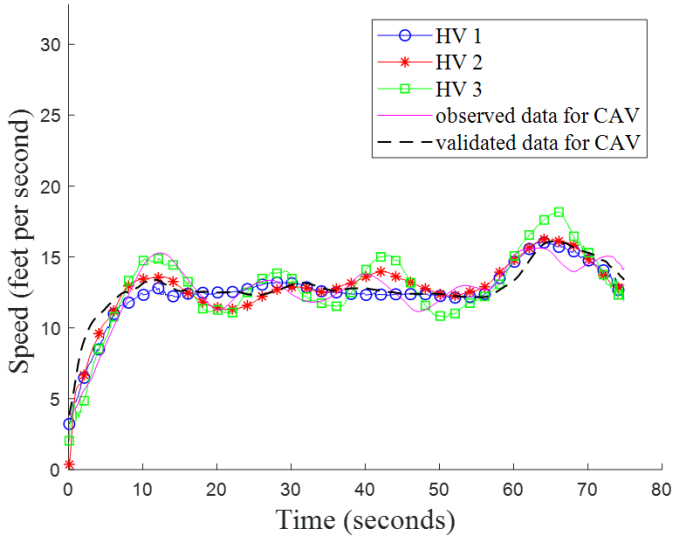

CAV = connected and automated vehicle.
HV = human-driven vehicle.
LC = lane changing.
Source: FHWA.

(b) Vehicle speeds in case 4.

Figure 11. Graph. Validation results of case 4.

REFERENCE

Wang, Z., Zhao, X., Xu, Z., Li, X., Qu, X., 2020. Modeling and Field Experiments on Lane Changing of an Autonomous Vehicle in Mixed Traffic. Computer-aided Civil and Infrastructure Engineering.